AUTOMATIC CLASS MEAN CALCULATION OF ROAD SURFACE FROM IKONOS IMAGES USING FUZZY LOGIC AND PARTICLE SWARM OPTIMIZATION

A. Mohammadzadeh [a,*], M. J. Valadan Zoej [a], A. Tavakoli [b]

[a] Geodesy and Geomatics Engineering Faculty, K.N.Toosi University of Technology, No. 1346, Vali_Asr St., Tehran, Iran, Postal Code: 1996715433 - ali_mohammadzadeh@alborz.kntu.ac.ir - valadanzouj@kntu.ac.ir
[b] Dept. of Electrical Engineering, Amirkabir University of Technology - tavakoli@aut.ac.ir

KEY WORDS: **Fuzzy logic, Particle swarm optimization, IKONOS, Road detection, Class Mean**

ABSTRACT:

Automatic road detection from high resolution satellite images has been an active research topic in the past decades. Different solutions are proposed to detect road object such as: fusion-based, fuzzy-based, mathematical morphology, model-based approach, dynamic programming and multi-scale grouping. In this paper, a new fuzzy segmentation method is proposed which is optimized by particle swarm optimization (PSO). The proposed method detects the road network using few samples from its surface. In the IKONOS images, the standard deviation of 10 grey level has been measured for the road classes. In the proposed fuzzy logic system, just one arbitrary pixel up to maximum of three from the road surface is an adequate initial value. The road is identified requiring neither the numbers of the classes nor the corresponding mean values. Particle swarm optimization is used to optimize the proposed fuzzy cost function. The proposed algorithm is applied on real IKONOS satellite image. The results indicate acceptable accuracy for the extracted road surface.

1. INTRODUCTION

Automatic detection and extraction of linear features especially road object has been the interest of many researchers for many years. Diverse solution has been proposed by researchers. Mena (2003) has presented a review of nearly 250 references on automatic road extraction. Furthermore, Zhang (2003), Mena and Malpica (2005), and Quackenbush (2004) have evaluated a wide variety of existing approaches. The applied road extraction methodologies could be summarized as follows (Mohammadzadeh et al., 2006):

(a) *Road tracking* methods start from a set of seed points and utilize radiometric values of pixels in the tracking process such as profile matching and Kalman filtering (Vosselman and DeKnecht, 1995; Bonnefon et al., 2002; Hu et al., 2004; Kim et al., 2004).
(b) *Morphological* methods rely on set theory developed by Matheron (1975) and Serra (1982). The method is sensitive to geometry of features and uses set operations such as union, intersection, complementation, dilation, erosion and thinning to identify geometrical characteristics of objects (Zhang et al., 1999; Amini et al., 2002a).
(c) *Snakes* along with *dynamic programming* is used for extraction of cultural structures such as roads and buildings (Agouris et al., 2001a, b; Péteri et al., 2004). Dynamic programming provides an optimized solution to road model Gruen and Li (1995). Simultaneous use of snakes and dynamic programming is reported by Gruen and Li (1997).
(d) *Artificial intelligent* approaches do reasoning based on the rules and models like a human being to provide correct, flexible and effective results. Fuzzy logic, neural networks and genetic algorithms are the most popular mathematical tools used in artificial intelligent systems. Fuzzy Logic (Zadeh, 1965) is a multivalued logic that allows intermediate values to be defined between zero and one (Agouris et al., 1998; Amini et al., 2002b). Artificial neural networks simulate the learning process of the human brain (Doucette et al., 2001; Egmont-Petersena et al., 2002) and genetic algorithms are generally used as an optimisation technique to search the global optimum of a function (Settea and Boullartb, 2001; Brumby et al., 1999).
(e) *Fusion-based* methods fuse multi-source and multi-type information (Jin and Davis, 2005; Chena et al., 2003; Pajares and de la Cruz, 2004). The information covers satellite images (visible and radar), domain-based models, expert's modeled knowledge, strategies and rules (Pigeon et al., 2001).
(f) *Multi-scale* along with *multi-resolution analysis* provide an efficient tool for road width detection and analysis of the road across profiles (Mayer et al., 1997; Mayer and Steger, 1998). Multi-resolution analysis is based on the topological relations between roads and other cartographic objects (Hinz et al., 2001; Chen et al., 2004; Hinz and Baumgartner, 2003).

In this research, new image segmentation based on fuzzy logic theory is proposed. Particle swarm optimization (PSO) has been employed to optimize the proposed approach. All of the classification and segmentation methods fell in two important groups: supervised and unsupervised methods. In supervised methods, necessary and enough samples should be selected from most of the possible classes in the image. In this way, classification parameters, like classes' mean and standard deviations are calculated from those selected sample data. The final result of the classification is highly affected by the selected samples and number of the user defined classes. In unsupervised methods, the user must define number of the classes or other equivalent parameters like minimum distance between the classes. But in the proposed method, just one up to three samples from the road surface is sufficient to calculate the mean value of class "road" in the image. Number of the classes and parameters of all the existing classes are not needed. This is an interesting advantage comparing to the previous classification and segmentation methods. By taking different samples from different images, the standard deviation of the road is found to be $\sigma = 10$. It is due to this fact that road surface is mostly homogenous and high radiometric variations are not expected. To see the efficiency of the method, it is applied on both simulated and real pansharpened IKONOS satellite image.

2. FUZZY SEGMENTATION OPTIMIZED BY PSO

Mohammadzadeh et al. (2006) proposed a new fuzy segmentation method, which computes road radiometric mean values in each ban using just few samples from its surface. In the proposed system, a blind search with one gray level accuracy in the search domain is performed to find the best mean value. The search domain is considered to be discrete and therefore few point are tested and there is fear of incorrect answers. Due to the mentioned reasons, a global minimum search approach should be applied to the proposed method. In addition, this will lead to a higher accuracy with sub gray level accuracy. In other words, PSO will find the global minimum of the fuzzy cost function with higher accuracy. Figure 1 illustrates the flowchart of the proposed algorithm.

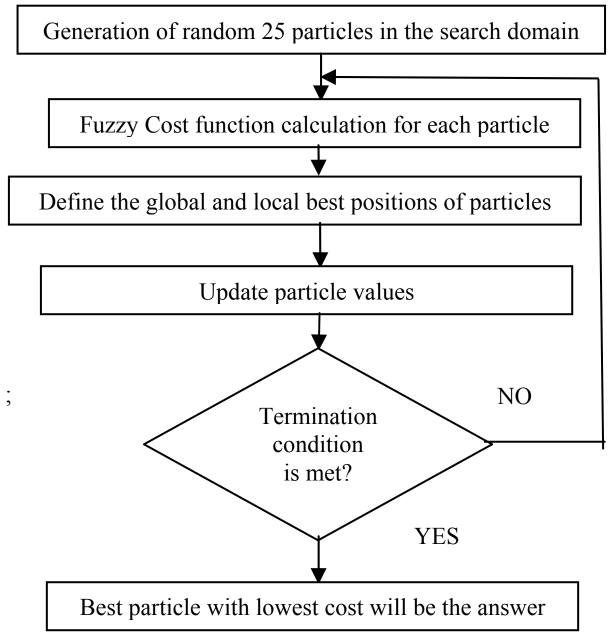

Figure 1. Flowchart of the method

The implemented PSO generates m=25 random particles in a continuous cubic search domain. Each of the particles has three values in the three dimensional search space, which are possible mean values of road in bands 1, 2, and 3. After taking few samples from the road surface, maximum and minimum values of particle 'm' in the band 'n' ($p_{m,n}^{old}$) will be defined as :

M : user selected sample pixel;

$M = [M_1, M_2, \ldots, M_n, \ldots, M_N]$: A pixel from the image

$\forall M_n \in X, \quad p_{m,n}^{old} = [(M_n - 15), (M_n + 15)] \quad ; n = 1,2,3$

Then the fuzzy cost function is evaluated for each of the produced particles. The particle that has the minimum cost value will be chosen as the best particle in each iteration. Then position of the particles will be updated based by the velocity vector which are influenced by both the best global solution associated with the lowest cost ever found by a particle and the best local solution associated with the lowest cost in the present population (see formulas 1 and 2). The best local solution replaces the best global solution if it has lower cost. The above procedure is carried out until the termination condition is met. For example, if differences of the two consequently calculated best mean values were below a user-defined threshold then the process will be finished and the last global best position would be considered as the final calculated best mean values of the road.

$$v_{m,n}^{new} = v_{m,n}^{old} + \Gamma_1 \times r_1 \times (p_{m,n}^{local\,best} - p_{m,n}^{old}) + \Gamma_2 \times r_2 \times (p_{m,n}^{local\,best} - p_{m,n}^{old}) \tag{1}$$

$$p_{m,n}^{new} = p_{m,n}^{old} + v_{m,n}^{new} \tag{2}$$

Where,

$v_{m,n}^{old} =$ *particle old velocity*

$v_{m,n}^{new} =$ *particle updated velocity*

$p_{m,n}^{old} =$ *particle old position*

$p_{m,n}^{new} =$ *particle updated position*

$r_1, r_2 =$ *independent uniform random numbers*

$\Gamma_1 = \Gamma_2 = 2$ *learning factor*

$p_{m,n}^{local\,best} =$ *best local solution*

$p_{m,n}^{global\,best} =$ *best global solution*

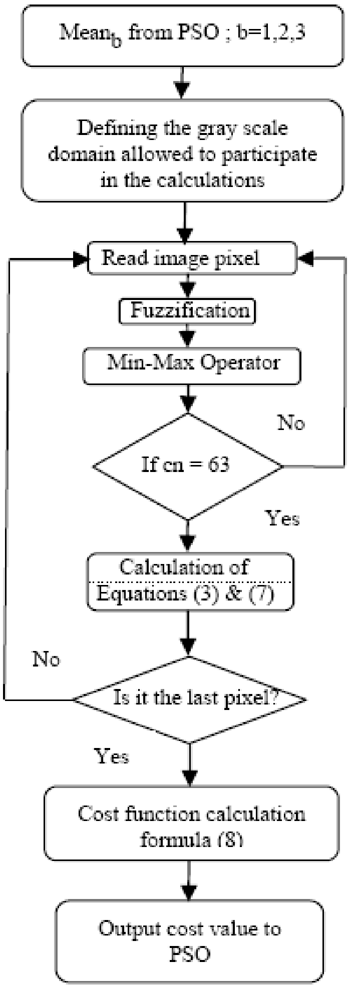

Figure 2. Flowchart of the fuzzy method

Figure 2 shows the flowchart of the implemented fuzzy system. The particle position as $p_{m,n}^{old}$ from the PSO method represents $mean_b \; ; b = 1,2,3$ which are the inputs of the fuzzy system. The pixels should satisfy the following criteria to participate in the fuzzy process:

$$X = [x_1, x_2, \ldots, x_b, \ldots, x_B] \text{; A pixel from the image} \qquad (3)$$
$$\forall x_b \in X, \quad (mean_b - 5.25 \cdot \sigma) \le x_b \le (mean_b + 5.25 \cdot \sigma) \quad ; b = 1,2,3$$

There are 5*5*5=125 possible fuzzy classes for three bands. Figure depicts the generated 5*5=25 classes in two bands.

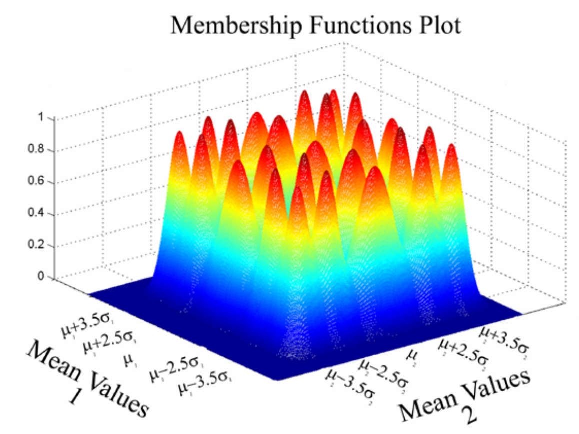

Figure 3. Defined classes using MFs of bands 1 and 2

Matrix F is calculated for each pixel of the image (see equation 4). The maximum among the minimum value of each column is found and its column number is attributed *"cn"*. If $cn \neq 63$, then the image pixel is considered as non-road.

$$f_{b,c}(x_b) = \exp\left(-\frac{(x_b - \mu_{b,c})^2}{2 * \sigma_{b,c}^2}\right) \Rightarrow f = [f_{b,c}]$$
$$\forall x_b \in [0,255] \quad \sum_{i=1}^{c=125} f_{b,i}(x_b) = 1 \qquad (4)$$

If *"t"* is the total number of initially identified road pixels, then for a pixel X_j where $1 \le j \le t$:

$$r_j = \begin{bmatrix} r_{1,1} \\ r_{2,1} \\ r_{3,1} \end{bmatrix}_{(M_j)} = \begin{bmatrix} (x_1 - \mu_{1,cn}) \cdot \left(\frac{1 - f_{1,cn}}{sum(f_{1,1:125})}\right) \\ (x_2 - \mu_{2,cn}) \cdot \left(\frac{1 - f_{2,cn}}{sum(f_{2,1:125})}\right) \\ (x_3 - \mu_{3,cn}) \cdot \left(\frac{1 - f_{3,cn}}{sum(f_{3,1:125})}\right) \end{bmatrix}_{(M_j)} \qquad (5)$$

$$sig\_cn = \begin{bmatrix} \sigma_{1,cn}^2 & 0 & 0 \\ 0 & \sigma_{2,cn}^2 & 0 \\ 0 & 0 & \sigma_{3,cn}^2 \end{bmatrix}$$

$$c_j = \sqrt{r_j \cdot inv(sig\_cn) \cdot r_j^T} \Rightarrow \quad sum\_c = \sum_{j=1}^{t} c_j \qquad (6)$$

$$d_j = \sum_{b=1}^{3} \left(1 - \frac{f_{b,cn}}{sum(f_{b,1:125})}\right)^2 \Rightarrow \quad sum\_d = \sum_{j=1}^{t} d_j \qquad (7)$$

This procedure is applied to all image pixels (or a selected window) and the cost function is calculated as:

$$Cost\_mean = \frac{sum\_c}{sum\_d \cdot t} \qquad (8)$$

The value of 'cost_mean' will be sent back to the PSO algorithm as the cost value for a particle like $p_{m,n}^{old}$.

3. IMPLEMENTATION AND RESULTS

Four simulated patterns are generated with hypothetic mean and standard deviation values as defined in Table 1 and is shown Figure 4. Table 2 shows the computed mean values for the simulated patterns using the proposed fuzzy-PSO method. The sub gray level difference between the computed mean values and the corresponding hypothetic ones indicate the efficiency and accuracy of the proposed method.

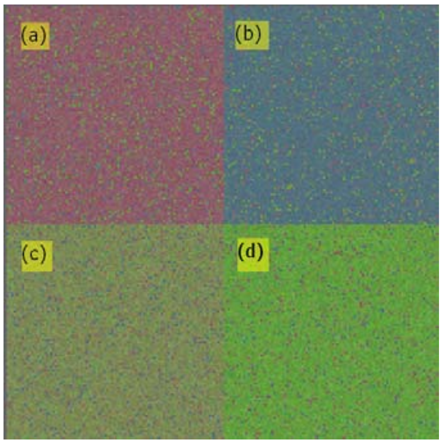

Figure 4. Simulated patterns (a) to (d).

Table 1. Hypothetic values used for pattern generation.

Pattern	Band 1 (grey level) μ_1	Band 1 (grey level) σ_1	Band2 (grey level) μ_2	Band2 (grey level) σ_2	Band3 (grey level) μ_3	Band3 (grey level) σ_3
Pattern (a)	140.3	6	93.2	9	104.8	8
Pattern (b)	82.7	7	113.7	6	125.9	4
Pattern (c)	123.3	8	137.5	10	86.4	7
Pattern (d)	98.7	10	158.3	9	63.1	6

Table 2. Computed mean values.

Pattern	Band 1 (grey level) μ_1	Band2 (grey level) μ_2	Band3 (grey level) μ_3
Pattern (a)	139.90	93.23	104.82
Pattern (b)	82.98	113.29	125.88
Pattern (c)	123.79	137.87	86.18
Pattern (d)	98.98	157.95	62.94

Figure 5 shows a window of 595*425 pixels from a pan-sharpened IKONOS image of Kish Island in Iran. In large scenes the road surface would be itself consist of two or three subclasses. Two subclasses were identified using the proposed methodology. The first arbitrary input sample was (63, 81, 77) and the calculated road mean for the first subclass was (68.30, 90.45, 85.06). The second arbitrary input sample was (100, 120, 100) and the calculated road mean for the first subclass was (93.66, 109.72, 95.79). The result of applying the proposed method is shown in Fig. 6.

Figure 5. IKONOS pan-sharpened image

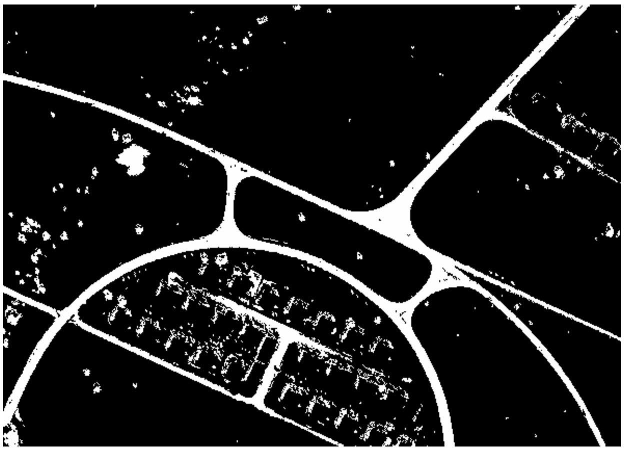

Figure 6. Detected road surface using fuzzy-PSO method.

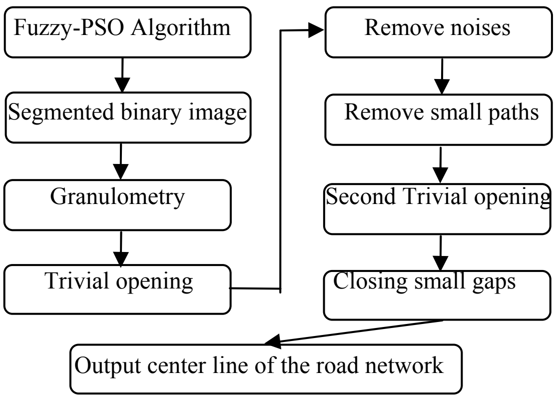

Figure 7. Block diagram used in morphology approach

Mohammadzadeh et al. (2004) extract road centreline based on mathematical morphology. Figure 7 shows the block diagram used in mathematical morphology. Mathematical morphology is non-linear image processing tool, which is sensitive to the objects shape. As roads appear as elongated narrow object in the image, therefore it is suitable to use mathematical morphology to extract road centreline. After applying the mentioned morphological algorithm, the final extracted road is shown in figure 8.

(a) result of trivial opening

(b) Closing operation

(c) result of opening

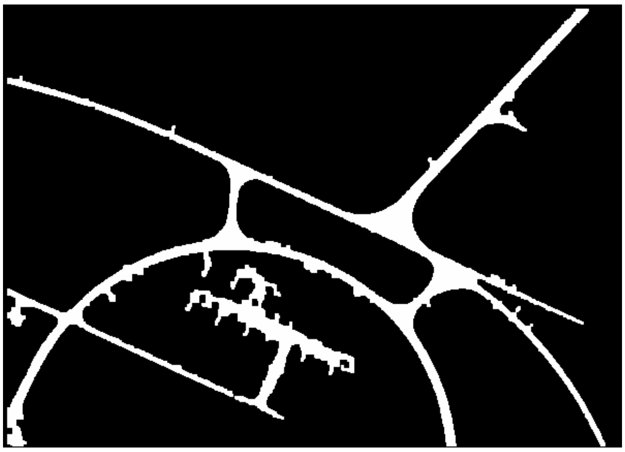

(d) applying second trivial opening

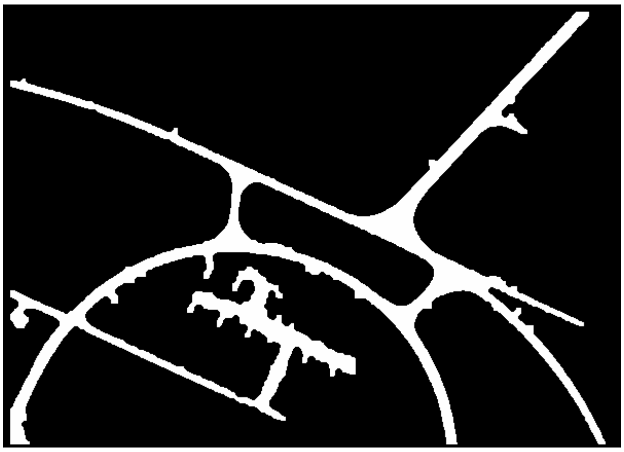

(e) second closing operator

(f) extracted road centerline

Figure 8. Road extraction from pan-sharpened IKONOS image of a rural area of *Kish* island: (a) result of trivial opening, (b) closing operator, (c) result of opening operation, (d) applying second trivial opening, (e) second closing operator, and (f) extracted road centerline in red which is superimposed on the original image.

4. CONCLUSIONS

The proposed fuzzy-PSO approach calculates the road's mean values automatically in different bands by using one up to three samples from the road surface with sub grey level accuracy. It is tested on both simulated and high resolution satellite images. Mathematical morphology is used to extract the road centerline. We should consider that the standard deviation of the road class is considered $\sigma = 10$ according to different sample we had from different IKONOS images. It is due to this fact that road appear as homogenous surface in the satellite images and so we do not expect high variance in the road surface reflectance data. The proposed algorithm shows a promising result. But one of our future efforts is to find a solution to obtain the exact standard deviation of the road surface from the satellite image in an automatic manner to achieve a more reliable detection algorithm. This would also lead us to detect other planimetric objects.

5. REFERENCE

Agouris, P., Gyftakis, S. and Stefanidis, A., 1998. Using a fuzzy supervisor for object extraction within an integrated geospatial environment. *International Archives of Photogrammetry and Remote Sensing,* 32(3/1):191-195.

Agouris, P., Gyftakis, S. and Stefanidis, A., 2001a. Quality-aware deformable models for change detection. Proceeding of *IEEE International Conference on Image Processing (ICIP),* Thessaloniki, Greece. 2: 805–808.

Agouris, P., Stefanidis, A. and Gyftakis, S., 2001b. Differential Snakes for Change Detection in Road Segments. *Photogrammetric Engineering & Remote Sensing,* 67(12): 1391-1399.

Amini, J., Saradjian, M.R., Blais, J.A.R., Lucas, C. and Azizi, A., 2002a. Automatic road side extraction from large scale image maps. *International Journal of Applied Earth Observation Geoinformation,* 4(2): 95–107.

Amini, J., Lucas, C., Saradjian, M.R., Azizi, A. and Sadeghian, S., 2002b. Fuzzy logic system for road identification using Ikonos images. *Photogrammetric Record*, 17(99): 493-503.

Bonnefon, R., Dherete, P. and Desachy, J., 2002. Geographic information system updating using remote sensing images. *Pattern Recognition Letter*, 23 (9): 1073-1083.

Brumby, S. P., Perkins, S. J., Theiler, J., Szymanski, J. J., Bloch, J. J., and Mitchell, M., 1999. Investigation of image feature extraction by a genetic algorithm. *Proceedings of the International Society for Optical Engineering, SPIE 3812,* Bellingham. Pages: 24-31.

Chen, T., Wang, J., Zhang, K., 2004. A Wavelet Transform Based Method for Road Centerline Extraction. *Photogrammetric Engineering & Remote Sensing*, 70(12): 1423-1432.

Chena, C.-M., Hepnerb, G.F. and Forster, R.R., 2003. Fusion of hyperspectral and radar data using the HIS transformation to enhance urban surface features. *ISPRS Journal of Photogrammetry & Remote Sensing,* 58(1-2): 19–30.

Doucette, P., Agouris, P., Stefanidis, A. and Musavi, M., 2001. Self-Organized Clustering for Road Extraction in Classified Imagery. *ISPRS Journal of Photogrammetry and Remote Sensing*, 55(5-6): 347-358.

Egmont-Petersena, M., De Ridderb, D. and Handelsc, H., 2002. Image processing with neural networks-a review. *Pattern Recognition,* 35(10): 2279–2301.

Gruen, A. and Li, H., 1995. Semi-automatic road extraction by dynamic programming. *ISPRS Journal of Photogrammetry and Remote Sensing,* 50(4):11-20.

Gruen, A. and Li, H., 1997. Semi-automatic linear feature extraction by dynamic programming and LSB-Snakes. *Photogrammetric Engineering & Remote Sensing,* 63(8): 985-995.

Hinz, S. and Baumgartner, A., 2003. Automatic extraction of urban road networks from multi-view aerial imagery. *ISPRS journal of photogrammetry & remote sensing*, 58(1-2): 83-98.

Hinz, S., Baumgartner, A., Mayer, H., Wiedemann, C., Ebner, H., 2001. Road extraction focusing on urban areas. *Automatic Extraction of Man-Made Objects from Aerial and Space Images (III)* (Eds. Baltsavias, E., Gruen, A. and Van Gool, L.). Balkema Publishers, Rotterdam, 415 pages: 255-265.

Hu, X., Zhang, Z. and Tao, C.V., 2004. A Robust Method for Semi-Automatic Extraction of Road Centerlines Using a Piecewise Parabolic Model and Least Square Template Matching. *Photogrammetric engineering and remote sensing,* 70(12): 1393-1398.

Jin, X. and Davis, C.H., 2005. An integrated system for automatic road mapping from high-resolution multi-spectral satellite imagery by information fusion. *Information Fusion,* 6(4): 257–273.

Kim, T., Park, S.-R., Kim, M.-G., Jeong, S. and Kim, K.-O., 2004. Tracking Road Centerlines from High Resolution Remote Sensing Images by Least Squares Correlation Matching. *Photogrammetric engineering and remote sensing*, 70(12): 1417-1422.

Matheron, G., 1975. Random set and integral geometry. John Wiley & Sons Inc., New York. 288 pages.

Mayer, H., Laptev, I., Baumgartner, A. and Steger, C., 1997. Automatic road extraction based on multi-scale modeling, context and snakes. *International Archives of Photogrammetry and Remote Sensing*, 32(3-2W3):106-113.

Mayer, H. and Steger, C., 1998. Scale-space events and their link to abstraction for road extraction. *ISPRS Journal of Photogrammetry and Remote Sensing,* 53 (2): 62– 75.

Mena, J.B., 2003. State of the art on automatic road extraction for GIS update: a novel classification. *Pattern recognition letters*, 24(16): 3037-3057.

Mena, J.B. and Malpica, J.A., 2005. An automatic method for road extraction in rural and semi-urban areas starting from high resolution satellite imagery. *Pattern Recognition Letters*, 26(9): 1201–1220.

Mohammadzadeh, A., Tavakoli, A., Valadan Zoej, M.J., 2004. Automatic linear feature extraction of Iranian roads from high resolution multi-spectral satellite imagery. *International Archives of Photogrammetry and Remote Sensing*, Istanbul, Turkey, PS ThS 12: Automated Object Extraction and Computer Vision Application, July, 13:30 - 15:30.

Mohammadzadeh, A., Tavakoli, A., Valadan Zoej, M.J., 2006, “Road extraction based on fuzzy logic and mathematical morphology from pan-sharpened IKONOS images”, The photogrammetric record, Vol. 21 (113):44-60.

Pajares, G., De la Cruz, J.M., 2004. A wavelet-based image fusion tutorial. *Pattern Recognition*, 37(9): 1855– 1872.
Péteri, R., Couloigner, I. and Ranchin, T., 2004. Quantitatively Assessing Roads Extracted from High-Resolution Imagery. *Photogrammetric Engineering & Remote Sensing,* 70(12): 1449–1456.

Pigeon, L., Solaiman, B., Toutin, T. and Thomson, K., 2001. Linear planimetric feature domains modeling for multisensor fusion in remote sensing. *Proceedings of SPIE Aero Sense 2000. SPIE,* 4051. 8 pages (CD-ROM).

Quackenbush, L. J., 2004. Review of Techniques for Extracting Linear Features from Imagery. *Photogrammetric engineering and remote sensing,* 70(12): 1383-1392.

Serra, J., 1982. *Image analysis and mathematical morphology.* Academic Press, London. 610 pages.

Serra, J. and Vincent, L., 1992. An overview of morphological filtering. *Circuits, Systems and Signal Processing.* 11(1):47-108.

Settea, S. and Boullart, L., 2001. Genetic programming: principles and applications. *Engineering Applications of Artificial Intelligence*, 14(6): 727–736.

Vosselman, G. and De Knecht, J., 1995. Road tracing by profile matching and Kalman filtering. *Automatic Extraction of Man-Made Objects from Aerial and Space Images (*Editors: Gruen, A., Kuebler, O. and Agouris, P.). Birkhäuser, Basel, Switzerland. 321 pages: 265-274.

Zadeh, L.A., 1965. *Fuzzy sets. Inform. Control*, 8: 338-353.
Zhang, C., 2003. Updating of cartographic road database by image analysis. Ph.D. thesis, Institute of Geodesy and Photogrammetry, ETH Zurich. 188 pages.

Zhang, C., Murai, S. and Baltsavias, E. P., 1999. Road network detection by mathematical morphology. *Proceedings of ISPRS Workshop on 3D Geospatial Data Production: Meeting Application Requirements*, Paris, France. Pages: 185-200.